BOLTED TIMBER CONNECTIONS: PART II. BOLT BENDING AND ASSOCIATED WOOD DEFORMATION[1]

Philip E. Humphrey and *Larry J. Ostman*

Assistant Professor and Graduate Research Assistant
Department of Forest Products
Oregon State University, Corvallis, OR 97331

(Received May 1988)

ABSTRACT

Complete double-shear joints with a single bolt were tested in tension. Approximately 10 X-ray scans were made of each joint as it was progressively loaded to failure; in this way, bending and overall displacement of the bolts within the members could be quantified. Combining the above data with measured joint-slip values enables the penetration of the bolt into the surrounding wood to be calculated for all positions along the length of the bolt. In a preceding related study, the authors observed the mechanisms of deformation that occur in thin wood wafers around a round steel pin of a diameter identical to that of the bolts used in the present work. By combining this information on behavior mechanisms in the plane at right angles to the pin axis with the X-ray data for whole joints, wood behavior throughout the joint and reactions against the bolt along its length can be estimated. The above analysis is applied principally to joints with 75- × 75-mm wood main members, 75- × 37.5-mm wood side members, and a single 12.5-mm diameter bolt an an end-distance of seven diameters. Representative X-ray scans of joints manufactured with a range of steel side-member thicknesses and bolt diameters are also included. The techniques presented complement theoretical model predictions and thus may be used to aid in optimizing joint design.

Keywords: Bolted joints, bolt deflection, X-ray scanning, wood-deformation mechanisms.

INTRODUCTION

Observing the behavior of bolted joints as they are loaded to failure may help us to understand the mechanisms that affect their performance. This direct approach has received surprisingly little attention in past research compared to the use of theoretical numerical models on the one hand, and purely empirical approaches on the other. The former are limited somewhat by the complexity of the system that they endeavor to represent, whereas the latter lead to inefficiencies in design.

The approaches reported here primarily involve observation of material behavior that occurs as timber joints with single bolts are loaded to failure in tension, and the use of derived data to predict distributions of deformation and reaction within the joints. Preceding complementary work carried out by the authors (Humphrey and Ostman 1989) concerns the experimental modeling of material behavior in the plane perpendicular to the bolt's longitudinal axis. The technique used in that work was developed to provide a practical counterpart to theoretical numerical models (principally finite element analyses), which necessarily make simplifying assumptions about the complex mechanisms of deformation and their

[1] Paper 2418, Forest Research Laboratory, Oregon State University, Corvallis. Currently, L. J. Ostman is Quality Control Director, Michigan California Lumber Company, Camino, CA. Mention of trade names or commercial products does not constitute endorsement or recommendation for use by the authors or Oregon State University.

Wood and Fiber Science, 21(4), 1989, pp. 354–366

interaction. Similar limitations apply to theoretical models of behavior of such joints in the direction parallel to the bolt axis. Indeed, fewer attempts have been made to model the bending and overall displacement of bolts within loaded joints. Most of the models that have been developed depend in part upon analyses in the plane perpendicular to the bolt's longitudinal axis.

Kuenzi (1955) was among the first to attempt to model the complete behavior of all parts of joints. Incorporated were formulae for an elastic foundation theory developed by Hetenyi (1939, 1946), which was modified for use in bolted and nailed connections. Stluka (1960) adapted these theories for a wide range of joint types and experimentally validated many of his theoretical predictions.

Following their use of finite element algorithms to model behavior in the plane perpendicular to the bolt's axis, Wong and Matthews (1981) emphasized the need to extend the algorithms to account for behavior in all directions, but recognized the difficulties of so doing. Smith (1982) surveyed available models for dowel-type connectors and went on to propose an adaptation of these using finite elements, which did enable the distribution of load throughout joints to be approximated.

The mechanisms operative within bolted connections resemble, to some extent, those operative in nailed joints, which have received more attention. Foschi (1977) was pioneering in his use of various elastic and inelastic foundation theories, finite elements, and closed form solutions to model the interaction between wood and nail in lap shear arrangements. Much of this work was founded on adaptations of the European Yield Theory first established by Johansen (1949). Tokuda (1977) used an X-ray scanning method to measure the movement of nails within wood shear specimens; this procedure enabled the accuracy of predicted data to be evaluated. Jansson (1955) and Noren (1961) also used elasto-plastic models for pin-type connectors, but these were not directly applicable to bolted joints.

Examination of the shapes of bolts removed from tested joints does not account for intermediate stages during the loading cycle or elastic straightening when the bolt is removed from the tested joint. It is the main objective of the technique presented herein to measure bolt bending and overall displacement during loading so that behavior of material in joints can be quantified. X-ray scanning, which produces silhouettes of bolts within joints, was used for this purpose. Bolt displacement values were combined with measured joint-slip values to predict the movement of the bolt in the surrounding wood along the entire length of the bolt. Combining these data with load-slip data collected by Humphrey and Ostman (1989) in the related study, in which pins 12.5 mm in diameter were drawn through thin wood wafers, enables a picture of the distribution of wood deformation and failure mechanisms throughout the joint to be formed at any stage during the loading cycle. Because the primary thrust of this study has been the development and validation of an experimental technique (rather than the completion of an extensive investigation of all the factors that interact to affect joint behavior), only a limited range of candidate joint types was tested.

MATERIALS AND METHODS

Preparation of test specimens

Five of the joints tested were of the design represented as Fig. 1a [a single mild steel bolt 12.5 mm in diameter passing through three defect-free wood members

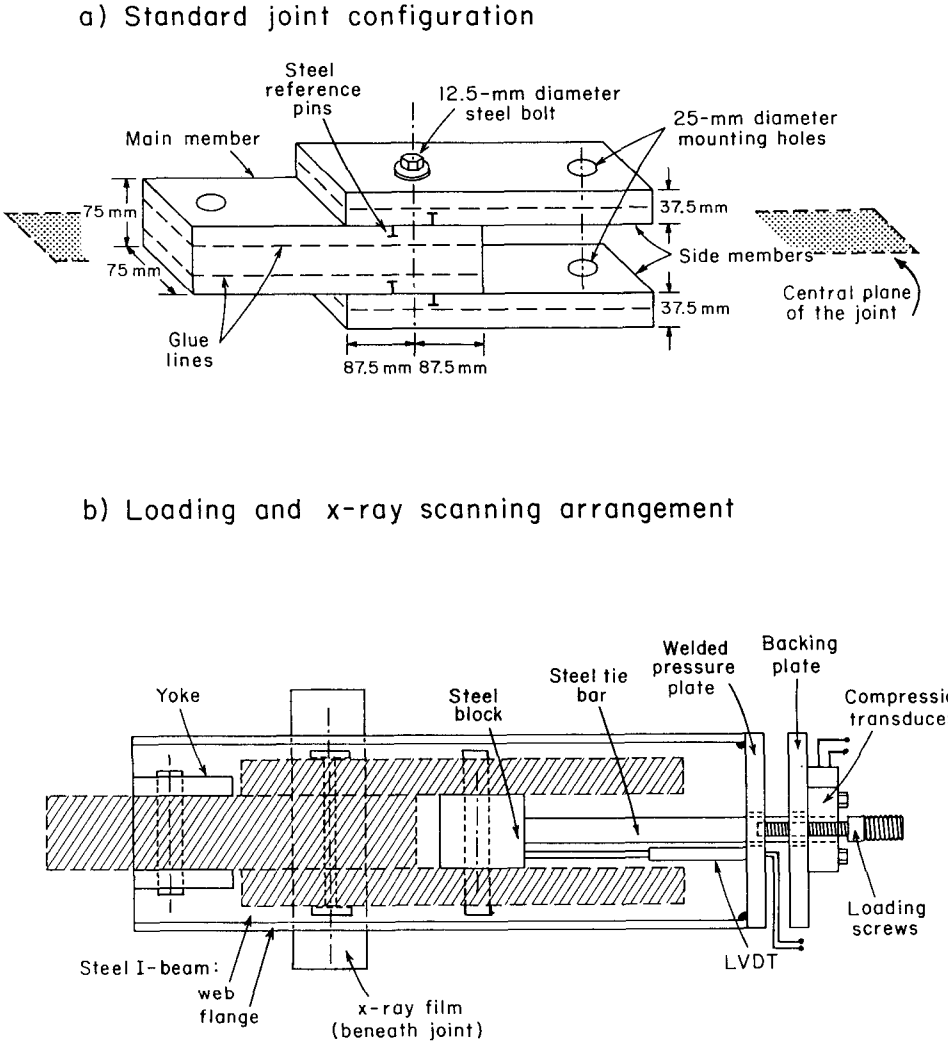

FIG. 1. a) Bolted joint configuration adopted as the standard for the investigation. The steel reference pins are used to infer total joint slip from the X-ray plates. b) Loading frame, with the standard joint in place (shaded), and principal elements of the X-ray scanning arrangement.

(a 75- × 75-mm main member and two 37.5- × 75-mm side members)]. Nuts were finger tight for all joints tested. This design has been adopted as a standard in the present work and will from here on be referred to as such.

Two factors influenced this choice of design. First, considerable experimental data have been accumulated on similar configurations (Stluka 1960; Wilkinson 1978; McLain and Thangjitham 1983), and some comparison of results may, therefore, be possible. Second, the joint arrangement was manageable on the available testing apparatus while lying within the range of bolt and member sizes used in commercial building systems.

Wooden joint members were cut from a glue-laminated beam 0.2 m wide × 1.1 m deep × 2 m long. Care was taken to ensure that the Douglas-fir [*Pseudotsuga*

menziesii (Mirb.) Franco] wood has growth characteristics and strength properties similar to those of the material from which the wafers used in the related study (Humphrey and Ostman 1989) were prepared. Members were conditioned to a moisture content of 12% (oven-dry basis) before being machined to final dimension within a tolerance of ±0.4 mm.

Intermember friction was not accounted for directly in the analysis reported here; it was therefore important to minimize variability in its influence among joints tested. For this reason, members were cut so that glue lines lay symmetrically within their cross sections to avoid exposing a glued surface at the shear plane between members, which would have affected the frictional coefficient between them (see Fig. 1a).

Bolt holes were cut with a specially ground drill bit, which produced smooth holes with a bolt clearance of 0.4 mm. Holes 25 mm in diameter also were drilled through the free ends of the members for mounting the joints in the testing arrangement. The position of these holes and the overall length of the members were influenced by the size of the loading frame and anticipated loads.

Matched pairs of cold-rolled mild steel plates, 75 mm wide but ranging in thickness (12.8, 6.4, and 2.0 mm), were also used as side members for some supplemental joints tested. The thickest plates (12.8 mm) remained undamaged after each test and could therefore be reused; the remainder distorted during testing and could be used only once. The steel side members were drilled with bolt and mounting holes equal in diameter to those of the wood side members (0.4-mm clearance).

Bolts of USS Grade 2 (SAE J429) were used throughout. This class of bolt is of low or medium carbon steel, is proof loaded to 390 MPa, and has a minimum yield strength of 404 MPa and a minimum tensile strength of 525 MPa. In addition to bolts 12.5 mm in diameter, a small number of extra tests were conducted with similar grade bolts 9.5 and 6.4 mm in diameter. These three bolt diameters correspond to effective bolt length to diameter ratios (L:D ratios) of approximately 12, 16, and 23, respectively. Washers were used beneath bolt heads and nuts in joints with wood side members.

Testing arrangement

Joint testing could not easily be conducted on a universal testing machine because X-rays had to be contained for safety. A rigid but portable loading frame capable of applying tensile loads up to 65 kN to joints in a controlled fashion was therefore designed. This frame was sufficiently compact to fit within a lead-lined cabinet 0.34 × 0.45 × 1.18 m, which also contained the X-ray scanning system (Fig. 1b).

The X-rays were produced by a self-rectified tube running at 60 kV and 7 mA. A narrow X-ray beam measuring 2 × 90 mm was collimated by interposing a specially slotted lead screen in the optical train. Once the rectangular (50- × 200-mm) pieces of X-ray film were placed in a recess beneath the joints, the bolts were scanned by driving the X-ray unit across the width of the joint with the aid of a lead screw and stepper motor. New pieces of film were placed beneath the joint for each scan as tensile loads on the joints were incrementally increased.

Relative movement between the ends of the main and side members of the joint (nominal joint slip) was measured during loading with a linear variable

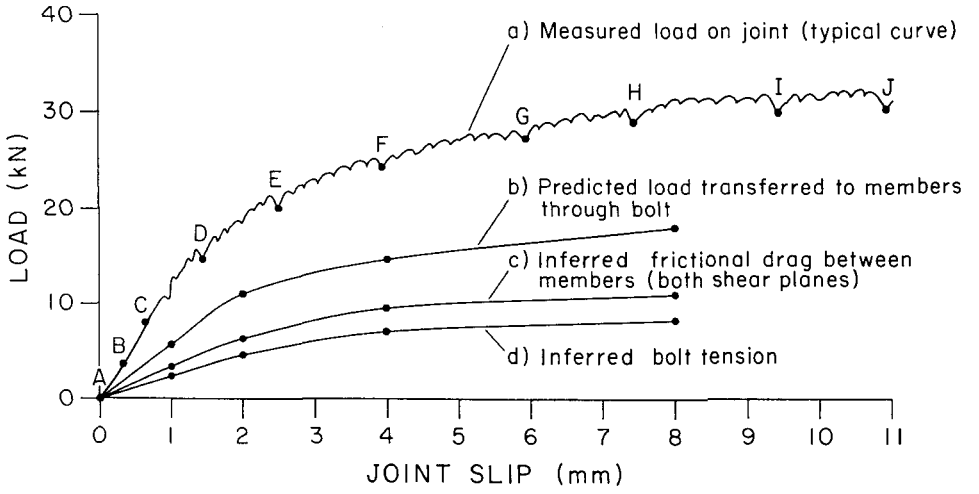

FIG. 2. a) A typical load-slip curve measured for a standard joint. Code letters A, C, E, G, and J correspond to the stages at which the selected X-ray plates in Fig. 3 were taken. b) Predicted load values transferred to members by the bolt (average of side- and main-member values). c) Inferred frictional drag between members (including both shear planes). d) Inferred tension in the bolt [derived by applying the measured static frictional coefficient (0.65) to predicted frictional drag values].

differential transformer (LVDT). In addition, joint slip values in the immediate vicinity of the bolts were captured on the X-ray film. The small steel reference pins positioned on the members (Fig. 1a) were visible on the X-ray images; this method of inferring slip values overcame the slight inaccuracies inherent in the LVDT data due to distortion of the loading frame and elastic deformation of the portions of the members extending beyond the immediate vicinity of the joint.

Tensile loads were transferred to the joint via a compact compression transducer. A steel tie bar 20 mm in diameter passed through the axially bored and threaded transducer, which was affixed to a backing plate. Two high-tensile machine screws that passed through threaded holes in the backing plate and acted on the pressure plate of the loading frame were used to effect loading. Axial alignment of the system was maintained when load was applied by turning the screws synchronously. An analog-to-digital data collection system operating at a sampling speed of 10 Hz was used to record load and nominal slip data for each joint tested.

Each joint was scanned before load was applied, and when it had been extended by approximately 0.3, 0.6, 1.2, 1.8, and 3 mm and then every 2 mm until it failed catastrophically. The joints were allowed to stand for 3 min after each incremental length increase and before scanning; this was time enough to allow the stress relaxation rate to fall sufficiently to avoid significant changes in bolt bending or position as the X-ray head moved along the length of the bolt (which took ap-

→

FIG. 3. Typical set of X-ray plates made while progressively loading a standard joint. Code letters correspond to the stages marked on the measured load-slip curve in Fig. 2.

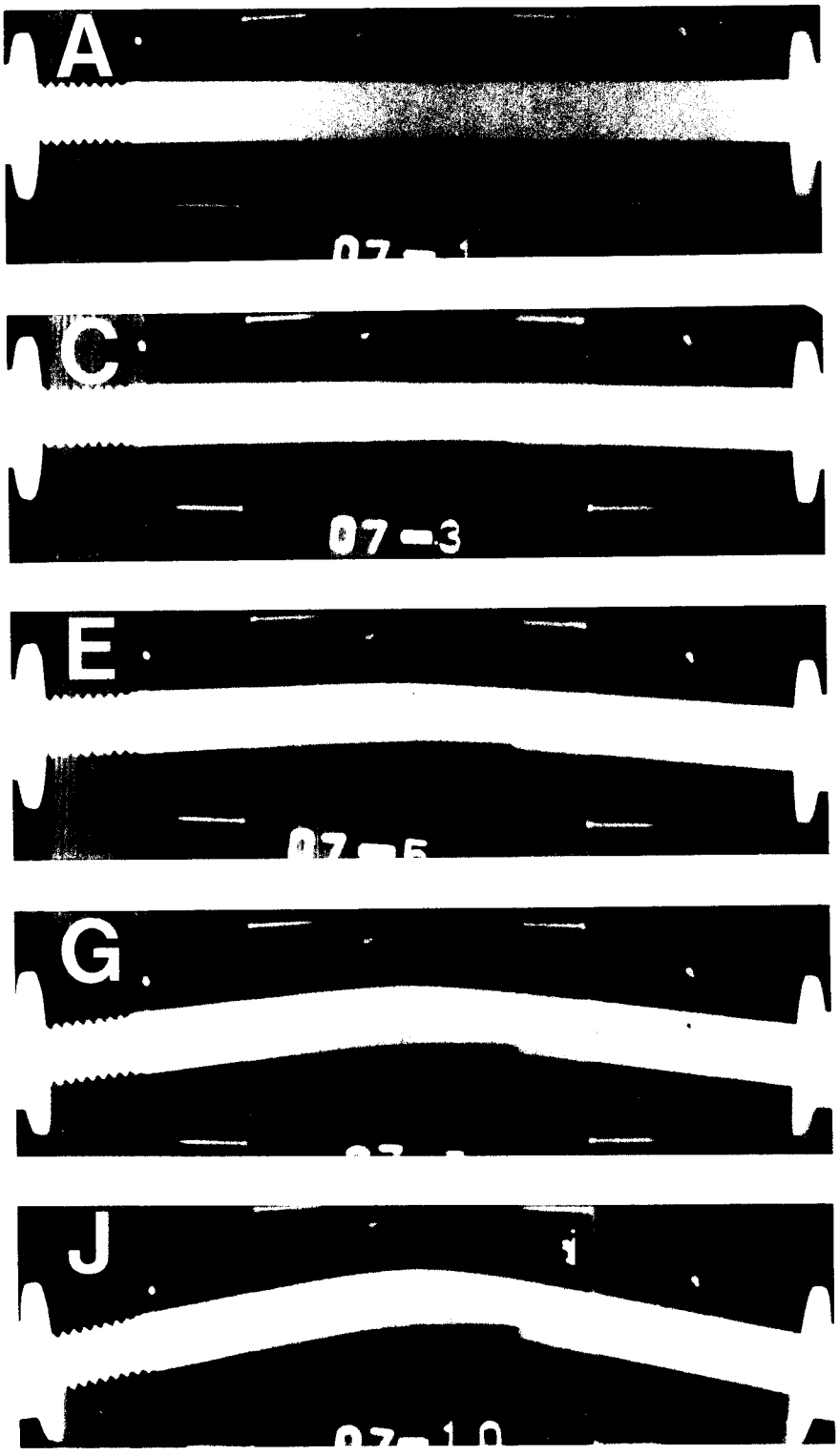
A
07-1
C
07-3
E
G
J

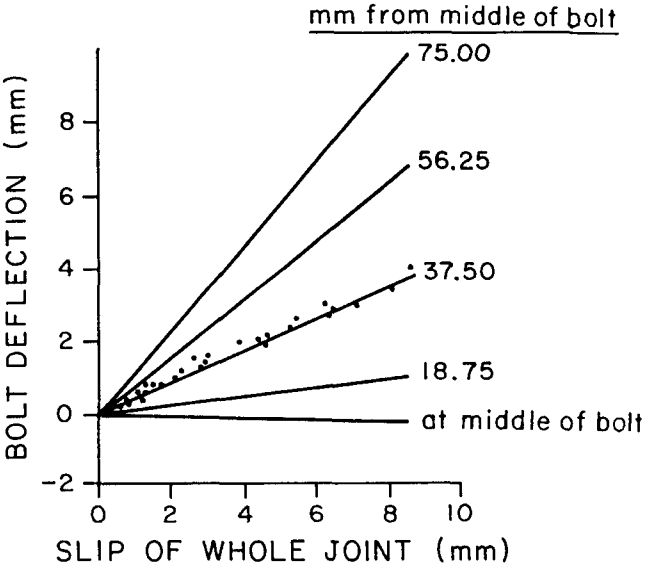

FIG. 4. Linearly regressed lines relating localized bolt displacement with joint slip, used for constructing averaged bolt-bending profiles. Each of the five plots corresponds to equally spaced positions across one-half of the width of the standard joint (one-half of bolt length); these data combine measurements from both halves of the five standard joints tested. For clarity, only one set of data points is included; scatter for the other four positions across the joint is similar.

proximately 5 sec). Each testing cycle (from initial loading to joint rupture) typically lasted 50 min; that is, the extension rate of the joint was approximately 0.25 mm/min when averaged over the entire testing sequence. Incremental extensions were applied at a rate of approximately 1 mm/min.

RESULTS AND DISCUSSION

Standard joint

A typical load-slip curve for a standard joint (see Fig. 1a) is shown as Fig. 2, curve "a," along with a representative set of corresponding X-ray scans as Fig. 3.

Constructing averaged bolt bending profiles.—Each developed X-ray plate was projected onto a screen with a photographic enlarger. Measurements were taken from sets of images for all five standard joints tested, which enabled the progressive change in bolt straightness and position relative to the main member to be ascertained. First, a reference line was established for each set of plates (derived from one joint). Then, eleven distances were measured on each plate, the first from the reference line to the reference pin of the main member, the remaining ten at equally spaced positions across the width of the joint (along the length of the bolt).

No significant difference could be detected (at the 5% exclusion level) between measurements taken at equal distances either side of the middle of the bolts in the standard joints. Natural variability within the wood material and the effect that this has on joint behavior appear to mask any asymmetry due to differences between bolt head and nut (known as bolt and fixity). Therefore, bolt bending

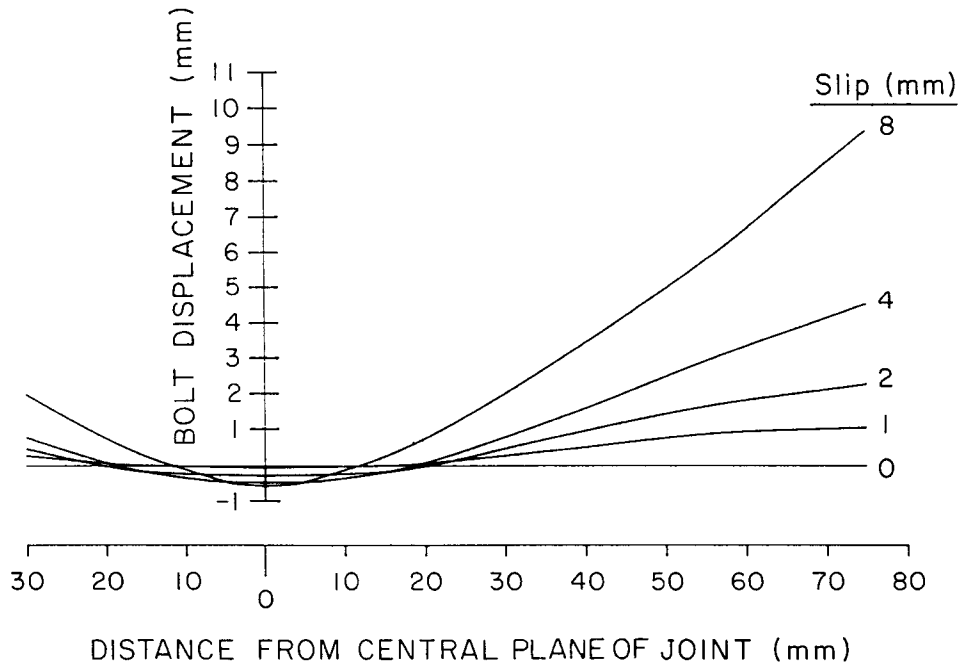

FIG. 5. Averaged bolt-bending profiles at five loading stages relative to a reference line on the main member, constructed from the regressed lines in Fig. 4.

could be assumed symmetrical about the central longitudinal plane of the joint (see Fig. 1a), and data for both sides of the joint were combined for analysis (standard joints only).

Joint slip values (movement between the side and main members extracted from the X-ray plates) were linearly regressed against localized bolt deflections for each of the five positions along one-half of the length of the bolt (Fig. 4). From these intermediate curves, averaged bolt deflections could be constructed for any joint slip level (Fig. 5). For this and the constructions to follow, a sign convention was established in which displacement in the direction of axial tensile loading of the main member is positive.

Modeling distributions of displacement and reaction.—Localized penetration of the bolt into the impinging wood may be inferred (Fig. 6) by combining measured joint-slip values (Fig. 4) with corresponding averaged bolt-bending profiles (Fig. 5). In this construction, allowance has been made for the 0.4-mm clearance between the bolt and hole. A small pre-load was applied to each joint to take up the clearance between the bolt and wood at the shear plane. However, as loading proceeded, bending of the bolt led to its movement across the clearance space. This transition may be seen toward the center of the main member and near the outer edges of each side member (see Fig. 6).

The distribution of localized reactions of the bolt against the impinging wood may be modeled (Fig. 7) at any stage in the loading cycle by combining inferred distributions of wood deformation (Fig. 6) with load-slip data measured in the related study by Humphrey and Ostman (1989) for wood wafers with correspond-

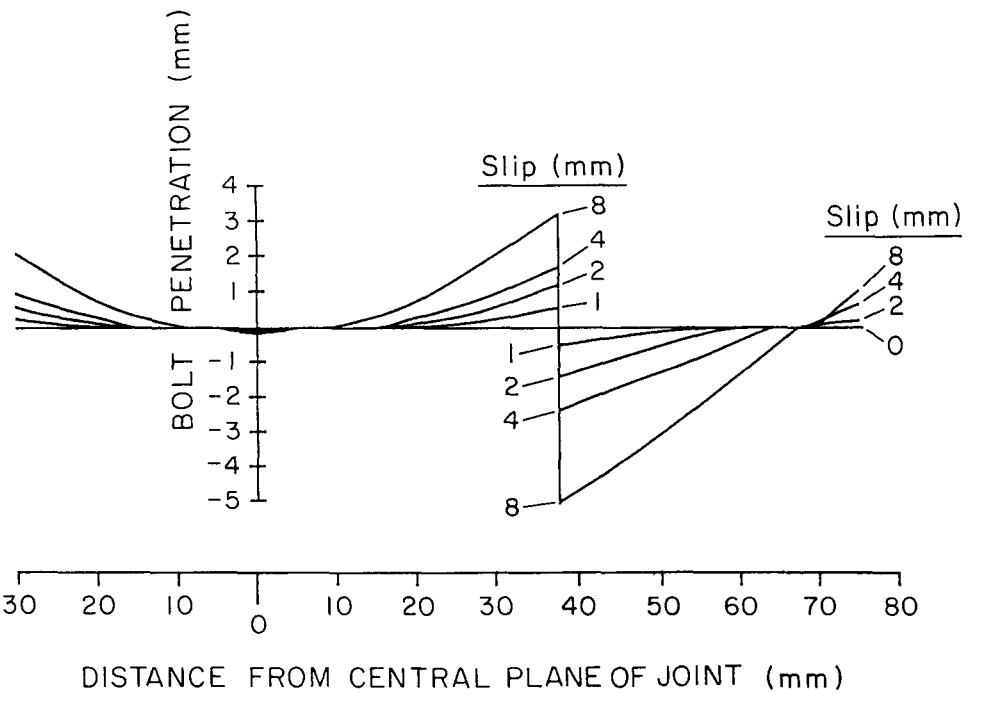

FIG. 6. Distributions of wood deformation at five loading stages, constructed by combining measured joint-slip values (Fig. 4) with corresponding averaged bolt-bending profiles (Fig. 5).

ing growth-ring orientation and geometry and a 12.5-mm diameter steel pin. For this purpose, the joint was subdivided into small (1.0-mm) transverse increments (along the length of the bolt) and the load supported over the width of each increment extracted from the load-slip curve derived by Humphrey and Ostman (1989). The curve shown in the Fig. 7 inset was obtained by combining and smoothing data measured for five similar wafers.

Integrating the areas under each load distribution curve in Fig. 7 enables total loads supported by the bolt on the wood foundation to be estimated. It is reasonable to expect that the integrated areas for the side and main members should sum to zero throughout the joint loading cycle and that any deviation from this condition reflects inaccuracies in the modeling method. Areas have been measured at the five stages of joint loading included in Fig. 7, converted to equivalent loads, and averaged (Table 1) for comparison with data collected for whole joints.

Frictional resistance and bolt tension.—Friction at the shear planes between the main and side members also contributes to the resistance to slippage of bolted joints, but this was not measured directly. Nuts were only finger tight at the beginning of each test, but as the bolts bent, tensile loads were created that led to the frictional resistance to joint slippage. If the modeled distribution of reactions against the bolt were perfectly accurate, then it should be possible to predict the partition of load between frictional drag and internal stress accommodation. To demonstrate this approach, predicted total loads supported by the wood lying beneath the bolt (curve "b" of Fig. 2) have been subtracted from loads actually

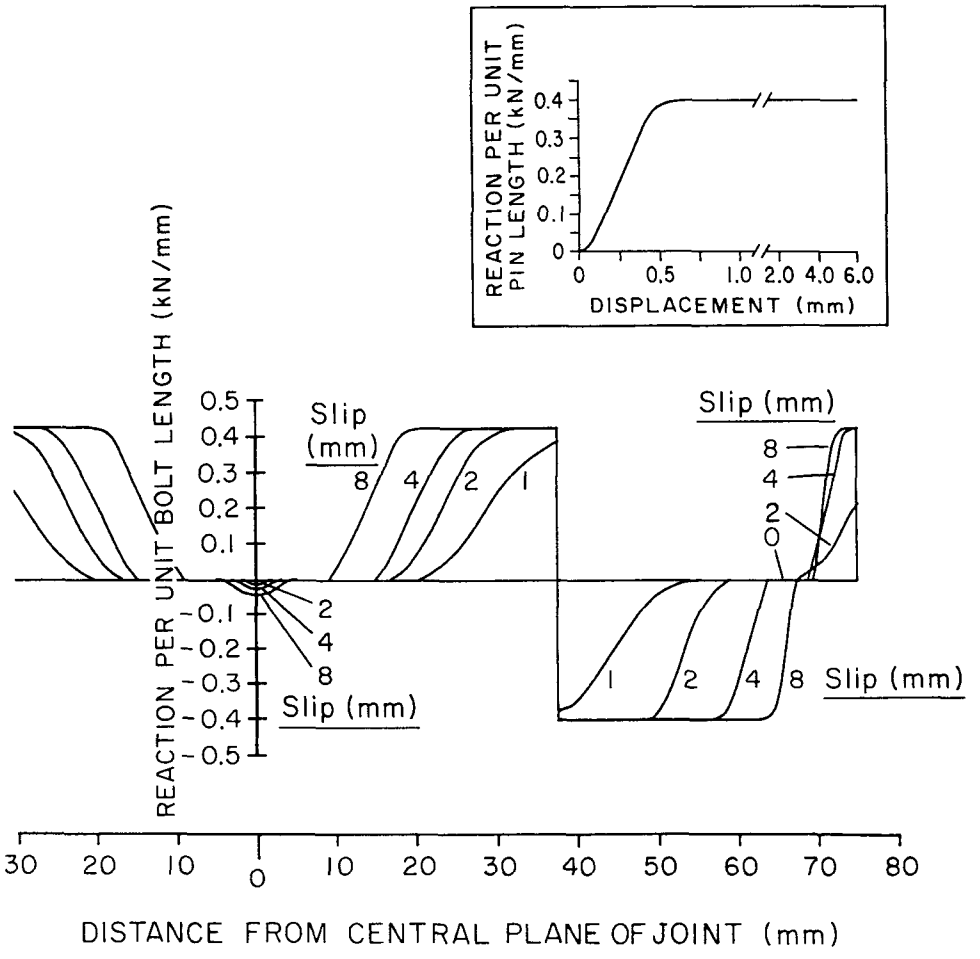

FIG. 7. Modeled load distribution along the length of the bolt at the joint loading stages selected for Figs. 5 and 6; constructed by combining distributions of wood deformation profiles with load-slip data for wood wafers [data generated with the wafer technique reported in the related study by Humphrey and Ostman (1989)]. Inset shows averaged and smoothed wafer load-slip curve used for constructing load distribution.

measured for the joint (curve "a" of Fig. 2); the resulting inferred frictional drag curve is shown as curve "c" of Fig. 2. These data are also included in Table 1 to clarify the sequence of numerical operations involved.

It is enlightening to estimate the tension that would be necessary in the bolt to result in such frictional values. For this purpose, the coefficient of dynamic (sliding) friction between the wood members was measured for a range of active loads from 10 to 40 kN/m^2 and a mean value of 0.65 was obtained. Inferred bolt-tension values are marked on Fig. 2 and are also included in Table 1. No attempt has been made to account for the differences between static and dynamic frictional coefficients. X-ray scans were not made frequently enough to enable the complex interaction among frictional coefficient, intermittent joint slippage (and consequent load relaxation), bolt bending, and associated bolt tension to be resolved.

TABLE 1. *Modeled and measured load values within the standard joint at a range of five slips.*

Joint slip (mm)	Modeled side-member load [each member][1]	Modeled main-member load [half width][1]	Averaged modeled member load [side and main members][2]	Measured joint load[2]	Inferred frictional drag [measured-modeled loads][2]	Inferred bolt tension [1/2 drag/frictional coeff.][2]
	(kN)					
0	0	0	0	0	0	0
1	2.76	3.17	5.93	10.05	4.12	3.17
2	5.39	5.54	10.93	18.80	7.87	6.05
4	7.40	6.88	14.28	24.50	10.22	7.86
8	8.94	9.36	18.30	29.90	11.60	8.92

[1] These values were obtained by integrating areas under the appropriate portions of the curves in Fig. 7.
[2] These values, presented here as part of a logical progression, also are shown in Fig. 2.

Inferred frictional drag values are much higher than those generally accepted for joints of this type. Clearly, care should be taken in interpreting the results because they are susceptible to all the deficiencies inherent in the modeling approach. Furthermore, although attempts were made to match the material used for the whole joints and the wafer tests (see Humphrey and Ostman 1989), differences did exist between them. Further work is planned to shed more light on the roles that frictional drag and bolt tension play in joint behavior. This will include the X-ray scanning of joints in which a low-friction membrane (such as PTFE) has been interposed between the members.

Supplemental joints

Representative bolt-bending profiles that developed during tensile loading of a range of supplemental joint designs are given in Fig. 8. The pairs of X-ray plates in Figs. 8a–d include the first (before loading) and the penultimate (just before failure) plates in the series; Figs. 8b and d also include a broken bolt. Though not analyzed in this study, these results are shown to provide a qualitative indication of the effects of bolt diameter (L:D ratio) and steel side-member thickness on bolt deformation.

Clearly apparent (particularly in Fig. 8a) are the effects of the greater restraint to bolt bending offered by the steel, compared to wood, side members. Resistance to rotation is offered in part by the rigid foundation lying beneath the head and nut (bolt and fixity), and this resistance is a function of bolt tension. Also of importance is the restraint imparted to the bolt by the rigidity of the walls of the holes passing through the steel members. As would be expected, these effects are greatest for the thickest side members (12.8 mm), and become most visible when these members are used in concert with the thinner bolts (Figs. 8b and d).

Thinner metal side members tended to provide a less rigid foundation for the nut and bolt heads and distorted as the wood around the bolt hole yielded to localized transverse stress concentration. Consequently, these joints sustained far greater slip values before failure than their counterparts with thicker plates, as evidenced by significantly greater bolt bending (Fig. 8c).

All joints with 12.5-mm diameter bolts failed within the wood members. When smaller diameter bolts were used, however, the bolts themselves failed as a result of combined tension and bending forces within them, and two X-ray plates have

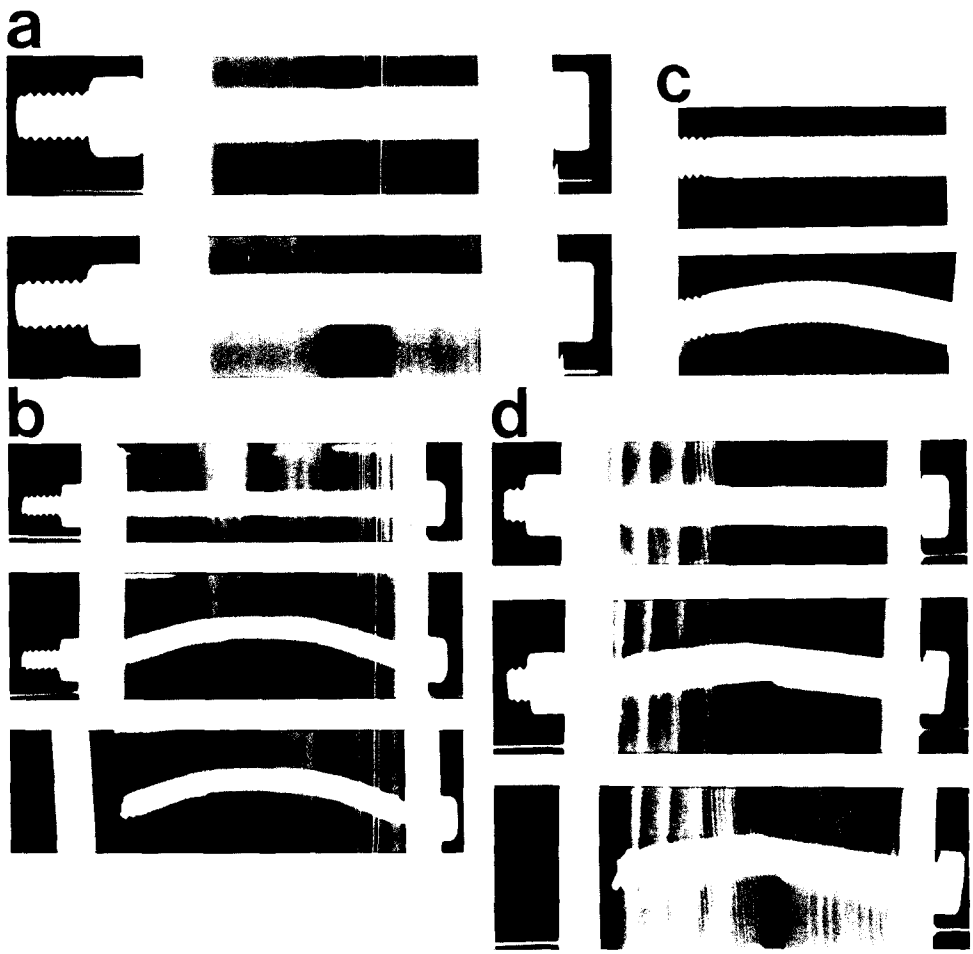

FIG. 8. Representative X-ray plates for supplemental joints manufactured with steel side members of varying thicknesses and bolts of varying diameters: a) thickness = 12.8 mm, diameter = 12.5 mm; b) thickness = 6.4 mm, diameter = 6.4 mm; c) thickness = 2.0 mm, diameter = 12.5 mm; and d) thickness = 6.4 mm, diameter = 9.5 mm.

been included to show such joints (side member, 6.4 mm thick; bolt diameters, 6.4 and 9.5 mm) immediately before and after bolt failure (Figs. 8b and d).

IMPLICATIONS

The main objective of the research reported herein, and that in the related study by Humphrey and Ostman (1989), has been to develop two complementary experimental techniques (X-ray scanning to quantify bolt bending and wafer testing for modeling wood deformation around bolts) and demonstrate their usefulness as tools to aid in efficient joint design.

The increasing quantity of portable and safe X-ray scanning equipment to be found in engineering and materials testing laboratories makes its widespread use for remote measurement of deformation within structural connections viable.

Data derived from scanning joints as they are progressively loaded may be used in three ways: 1) directly, to indicate the relative significance of contributory mechanisms that affect system behavior, 2) to enable the quality of numerical simulation models (such as those using finite element analysis and closed form solutions) to be gauged before they are selected as design tools, and 3) to provide data that may be incorporated in rather less fundamentally based modeling methods like the one described here.

The application of techniques that employ methods of direct observation may prove most useful when addressing the complex effects of wood quality, growth defects such as knots in the immediate vicinity of joints, fabrication tolerances, and combined loading. Indeed, unidirectional and combined loading (simultaneous application of tension and bending forces) of multiple-bolt joints is the subject of ongoing research at Oregon State University. Duration of load and effects of environmental conditions (principally moisture content and temperature) must also be addressed, and methods such as those described herein may aid in this endeavor.

REFERENCES

FOSCHI, R. O. 1977. Load-slip characteristics for connections with common nails. Wood Sci. 9(3): 118–123.

HETENYI, M. 1939. Analysis of bars on elastic foundations. Int. Assoc. Bridge Struct. Eng. Second Congress, Wilhelm Ernst and John, Berlin-Munich.

———. 1946. Beams on elastic foundations. University of Michigan Press, Ann Arbor, MI.

HUMPHREY, P. E., AND L. J. OSTMAN. 1989. Bolted timber connections: Part I. A wafer technique to model wood deformation around bolts. Wood Fiber Sci. 21(3):239–251.

JANSSON, G. B. I. 1955. Effect of nail characteristics on load-carrying capacity of a nailed joint. M.S. thesis, Iowa State College, Ames, IA.

JOHANSEN, K. W. 1949. Theory of timber connections. Int. Assoc. Bridge Struct. Eng. 9:249–262.

KUENZI, E. W. 1955. Theoretical design of a nailed or bolted joint under lateral load. USDA For. Serv. Rep. No. D1951. For. Prod. Lab., Madison, WI.

MCLAIN, T. E., AND S. THANGJITHAM. 1983. Bolted wood joint yield model. J. Struct. Div. ASCE 109(8):1820–1835.

NOREN, B. 1961. Nailed joints—a contribution to the analysis of yield and strength. Proceedings—First International Conference on Timber Engineering, Southampton, UK.

SMITH, I. 1982. Analysis of mechanical timber joints with dowel type connectors subjected to short term lateral loading—by finite element approximation. Res. Rep. 2/82. Timber Research and Development Association, Hughenden Valley, Buckinghamshire, UK.

STLUKA, R. T. 1960. Theoretical design of a nailed or bolted joint under lateral load. M.S. Thesis, Dept. of Civil Engineering, University of Wisconsin, Madison, WI.

TOKUDA, M. 1977. Studies on the nailed wood joint. I. Measurements of the nail shear deformation by Softex. Mokuzai Gakkaishi 23(1):17–24.

WILKINSON, T. L. 1978. Strength of bolted wood joints with various ratios of member thicknesses. USDA For. Serv. Res. Pap. FPL 314. For. Prod. Lab., Madison, WI.

WONG, C. M. S., AND F. L. MATTHEWS. 1981. A finite element analysis of single and two-hole bolted joints in fiber reinforced plastic. J. Compos. Mater. 15:481–491.